D. P. Updike

A. Kalnins

Department of Mechanical Engineering and Mechanics,
Lehigh University,
Bethlehem, PA 18015

S. M. Caldwell
Eastman Chemical Company,
Kingsport, TN 37662

Residual Stresses in Transition Zones of Heat Exchanger Tubes

A theoretical model of an expanded tube-to-tubesheet joint is developed and examined with the objective to determine the residual stresses in the transition zone, which lies between the expanded and unexpanded regions of the tube. Owing to their effect on the development of stress corrosion cracks, the residual tensile stresses on the surfaces of the tube are of particular interest. A mathematical model that can predict these residual stresses is developed. Results of the model show that the maximum tensile residual stresses are axial and occur on the inside diameter of the expanded tube. It is shown in a parameter study that, for expansions that ensure a leak-tight joint, the maximum residual tensile axial stress on the inside surface of the tube reaches 80–95 percent of the yield stress of the tube, regardless of the geometrical and material parameters of the tube and tubesheet.

1 Introduction

This paper is concerned with tubes that are expanded in a tubesheet of a heat exchanger or a condenser. Stress corrosion cracks have been observed in the transition zones between the expanded and unexpanded regions of tubes. One of the factors that influence the initiation and growth of such cracks is the residual tensile stress that is left in the tube by the expansion process. The objective of this paper is the development of a mathematical model from which the residual stresses in the transition zone can be determined for any set of tube and tubesheet parameters.

A number of papers have investigated the strength of the tube-tubesheet joint, with the emphasis on contact pressure, holding power, and tightness against leakage ([1–4]). The residual stresses in the transition zone of the tube, which is the objective of this paper, have received much less attention. Druez, Bazergui, and Pettigrew [5] did an experimental study. Aufaure, Boudot, Zacharie, and Proix [6] reported in-service cracks and presented theoretical and experimental results for the residual stresses. The photographs that are included in [6] show axial cracks on the inside diameter of the tube in the region that is adjacent to the uniformly expanded zone, which turn into circumferential cracks when going away from the uniformly expanded zone.

2 Tube Expansion Process

Tube-tubesheet joints can be expanded in a number of ways. We consider here the expansion by either a mechanical roller or by a hydraulic process. During the rolling process, shown schematically in Fig. 1, the tube is expanded by an expander, equipped with several rollers. During the first phase of the process, the initial clearance between the tube and the hole in the tubesheet is closed. During subsequent passes of the rollers, the tube wall is squeezed between the rollers and the rim of the hole, and the tubesheet is also expanded. When the expander is withdrawn, both the tube and the tubesheet spring back. The objective is to leave the tube in contact with the tubesheet after the springback. During hydraulic expansion, fluid pressure is applied within the tube to achieve the same objective. While the positive aspect of the process is the contact pressure between the expanded tube and the tubesheet, one negative side effect is the appearance of tensile residual stresses that may accelerate stress corrosion cracking.

The expanded tube can be divided into five different zones. They are shown in Fig. 2, displayed with respect to a calculated profile of the inside tube surface of an expanded tube. The zones are: 1) uniformly expanded zone; 2) toe, in which the axial bending is severe; 3) the taper, characterized by nearly uniform slope; 4) tail, in which reverse axial bending pre-

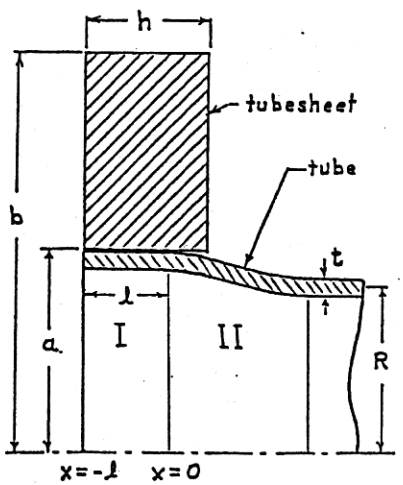

Fig. 1 Geometry of an expanded tube-tubesheet joint. I—expanded zone; II—transition zone.

Contributed by the Pressure Vessels and Piping Division for publication in the JOURNAL OF PRESSURE VESSEL TECHNOLOGY. Manuscript received by the PVP Division, November 26, 1990; revised manuscript received, January 13, 1992. Associate Editor: A. K. Dhalla.

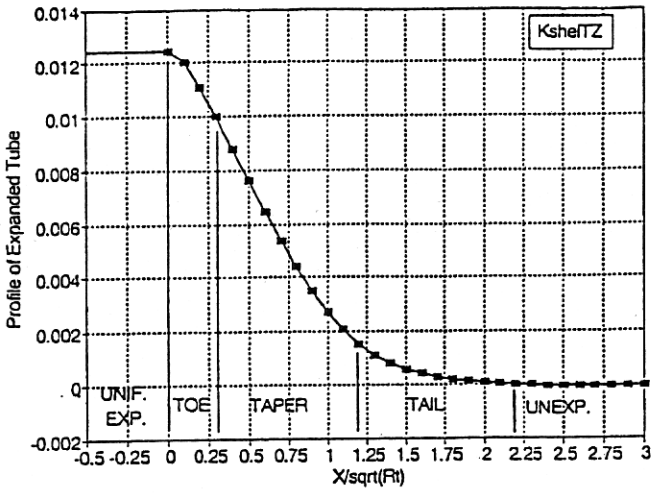

Fig. 2 Profile of expanded tube

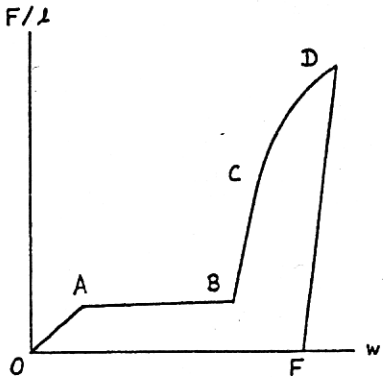

Fig. 3 Expansion loading versus radial displacement

dominates; and 5) unexpanded zone. The toe, taper, and tail make up what is called the transition zone.

What causes the residual stresses? Figure 3 shows schematically the expansion force for hydraulic expansion plotted versus the normal deflection of the inner surface of the tube within the uniformly expanded zone. Curve OAB describes the behavior while there is still clearance between the tube and the hole. The change in slope at point B is due to the added stiffness from expanding the tubesheet after contact is made. Curve BCD corresponds to expansion of the tube and tubesheet, with BC representing elastic behavior in the tubesheet and CD the elastic-plastic behavior, after a plastic zone develops around the hole. Curve DF represents the springback during unloading, when the expander is withdrawn. The residual displacement in the uniformly expanded zone is given by OF, while those in the unexpanded zone are zero. The mismatch of the residual displacements is responsible for the residual stresses in the transition zone.

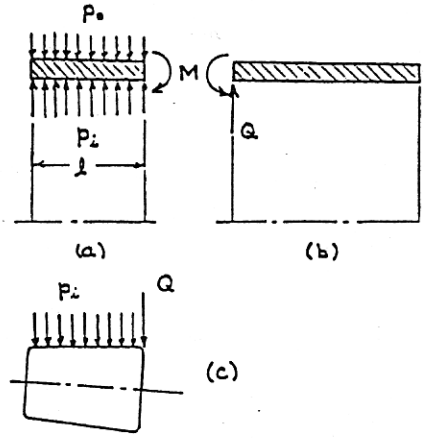

Fig. 4 Axisymmetric loading on tube and expander: (*a*) expanded zone; (*b*) transition zone; (*c*) expander

3 Validity of Model

The model developed in this paper makes three key assumptions: 1) axisymmetric deformation; 2) zero slope of the meridian at the junction of the toe and the uniformly expanded zone; and 3) the force distribution over the expander, consisting of a uniform pressure and a concentrated radial load, denoted by Q in Fig. 4. These assumptions were needed in the devel-

Nomenclature

Geometry

- a = radius of hole in tubesheet
- b = outer radius of sleeve model of tubesheet
- h = thickness of tubesheet
- l = length of contact with expander
- R = mean radius of tube
- t = thickness of tube
- r_i = $R-t/2$, inner radius of tube
- r_o = $R+t/2$, outer radius of tube
- d_o = outside diameter of tube
- d_i = inside diameter of tube
- t = thickness of tube
- c = $a-r_o$, initial radial clearance
- x = axial coordinate along tube
- r = radial coordinate
- θ = circumferential coordinate
- β = $1.285/\sqrt{(Rt)}$ shell parameter for tube
- m = apparent wall reduction

Material Properties

- E = Young's modulus of tube
- ν = 0.3, Poisson's ratio of tube
- Y = yield stress of tube
- E_{tan} = tangent modulus for plastic range of tube
- E' = Young's modulus of tubesheet
- ν' = 0.3, Poisson's ratio of tubesheet
- Y' = yield stress of tubesheet
- E'_{tan} = tangent modulus for plastic range of tubesheet

Solution Variables

- w = radial displacement of tube at mid-thickness
- u = radial displacement of tubesheet at hole
- p_i = pressure on inner surface of tube
- p_o = pressure on outer surface of tube
- N = compressive radial force per unit circumference at contact between tube and tubesheet
- F = radial force per unit circumference at contact between expander and tube
- Q = transverse shearing force per unit circumference at edge of transition zone
- M = bending moment per unit circumference at edge of transition zone
- $\sigma_x, \sigma_r, \sigma_\theta$ = components of stress
- $\epsilon_x, \epsilon_r, \epsilon_\theta$ = components of strain

Superscripts

- $\hat{}$ = value during expansion
- $\bar{}$ = change during springback
- $\tilde{}$ = residual value

mediate values of E_{tan}/E. Also, available from this data base are values of nondimensional stresses along the tube.

During springback purely elastic unloading is assumed. Let $\bar{Q}$, $\bar{M}$, and $\bar{w}$ be the changes in Q, M and w, respectively. For springback, the stiffness relations derived from edge-effect solutions for elastic semi-infinite cylindrical shells for $\nu = 0.3$ are

$$\bar{Q}\sqrt{(Rt)}/Yt^2 = 0.7780(E\bar{w}/YR) \tag{7}$$

$$\bar{M}/Yt^2 = 0.3026(E\bar{w}/YR) \tag{8}$$

4.4 Combined Behavior of Tube and Tubesheet During Load-Up. The loading on the tube parts has been previously shown in Fig. 4, while the loading on the tubesheet is the radial load N. Calculation of the behavior of the tube-tubesheet combination requires satisfying equilibrium of forces and matching of displacements. For equilibrium at contact between the expanded zone and the tubesheet the relation is

$$\hat{N} = \hat{p}_o l \tag{9}$$

The force per unit circumference provided by the expander is

$$\hat{F} = \hat{p}_i l + \hat{Q} \tag{10}$$

The displacement of the outer surface of the tube is found by adding the initial radial clearance to the displacement at the boundary of the hole. With the assumption that the displacement within the tube varies as $1/r$ through the wall of the tube in the expanded portion, one can now calculate the radial deflection w at mid-thickness using

$$\hat{w} = (\hat{u} + c)(1 + t/2R) \tag{11}$$

This value pertains to both the expanded zone and the edge of the transition zone.

The solution state at maximum outward displacement may be found in terms of a parameter which sets the severity of expansion. In the present work the contact pressure $\hat{p}_o$ is chosen for the parameter. The calculation procedure is then straight forward. First, $\hat{N}$ is found from (9), then $\hat{u}$ from the stored data base, then $\hat{w}$ from (11), then $\hat{Q}$ from the data base, then $\hat{p}_i$ from analysis of the expanded zone, and finally, $\hat{F}$ from Eq. (10).

4.5 Combined Behavior During Springback: Residuals. Let $\bar{p}_i$, $\bar{p}_o$, $\bar{Q}$, $\bar{N}$, $\bar{F}$, $\bar{w}$, and $\bar{u}$ be the changes in the various loads and displacements during springback, and $\tilde{p}_i$, $\tilde{p}_o$, $\tilde{Q}$, $\tilde{N}$, $\tilde{F}$, $\tilde{w}$, and $\tilde{u}$ be their residual values. The residuals are related to the maximums and the changes due to unloading through equations of the type

$$\tilde{p}_i = \hat{p}_i + \bar{p}_i; \quad \tilde{p}_o = \hat{p}_o + \bar{p}_o;$$
$$\tilde{Q} = \hat{Q} + \bar{Q}; \quad \tilde{N} = \hat{N} + \bar{N}; \quad \tilde{F} = \hat{F} + \bar{F};$$
$$\tilde{w} = \hat{w} + \bar{w}; \quad \tilde{u} = \hat{u} + \bar{u} \tag{12}$$

In the residual state, the edge shear $\tilde{Q}$ on the transition zone results from contact with the tubesheet, so that the radial load on the tubesheet becomes

$$\tilde{N} = \tilde{p}_o l - \tilde{Q} \tag{13}$$

The expansion loading is removed completely; thus

$$\tilde{F} = \tilde{p}_i l = 0 \tag{14}$$

Again, assuming that the radial displacement varies as $1/r$ through the thickness in the expanded zone gives

$$\bar{w} = \bar{u}(1 + t/2R) \tag{15}$$

Combining (12) and (14) gives

$$\bar{p}_i = -\hat{p}_i \tag{16}$$

Also, combining (13), (12), and (9) gives

$$\bar{N} = \bar{p}_o l - \hat{Q} - \bar{Q} \tag{17}$$

Equations (1), (6), (7), (15), (16), and (17) now form a linear system, which may be solved for the spring back variables $\bar{N}$, $\bar{p}_i$, $\bar{p}_o$, $\bar{Q}$, $\bar{u}$, and $\bar{w}$.

The springback solution is checked for possible yielding during unloading. If such yielding is detected, suitable corrections are made in the analysis.

4.6 Transition Zone Stresses. The stress distributions at the end of the loading process are available from the data base. The residual stresses are obtained by superposing on these stresses the additional stresses that occur during springback. The stress changes during unloading (springback) are calculated using the equations for discontinuity stresses in thin elastic shells. For Poisson's ratio equal to 0.3, the equations are

$$\bar{\sigma}_x/Y = \pm 1.816(E\bar{w}/YR)e^{-\beta x}(\cos\beta x - \sin\beta x) \tag{18}$$

$$\bar{\sigma}_\theta/Y = 0.3\bar{\sigma}_x/Y + (E\bar{w}/YR)e^{-\beta x}(\cos\beta x + \sin\beta x) \tag{19}$$

where $\beta x = 1.285x/\sqrt{(Rt)}$, $\bar{w}$ refers to the edge springback radial displacement (a negative quantity), and the lower and upper signs refer to the inside and outside surfaces, respectively. It may be noted that these expressions for the stresses show rapid attenuation with the parameter $x/\sqrt{(Rt)}$.

5 Selection of Nondimensional Parameters

5.1 Geometry and Material Parameters. For the calculations that follow, all geometric lengths are normalized with respect to the outer tube diameter, d_o. The thickness ratio, t/d_o, is used to characterize the tube geometry. All calculated stresses are normalized with respect to the yield stress of the tube, Y, which is defined as the stress at the point of discontinuity of the slope in an elastic-linearly strain-hardening model of the stress-strain curve. The two slopes of the curve are E in the elastic range and E_{tan} in the elastic-plastic range. Two nondimensional parameters, E/Y and E_{tan}/E, characterize the stress-strain curve for the tube material.

The tubesheet geometry makes use of an annulus model previously used in [2 and 3]. The annulus has an inner radius a, outer radius b, and thickness h. The annulus model assumes a traction-free boundary at the outer radius and depends on the tube spacing, or pitch, as determined in [8]. The nondimensional parameters which characterize the tubesheet geometry are the ratios b/a and $h/2a$.

It is assumed that the hole diameter, $2a$, is approximately equal to the tube outside diameter, and it accounts for the initial gap between the tube and the hole by introducing the parameter c, the radial clearance, such that $2c = 2a - d_o$. The nondimensional parameter for clearance is taken to be $2c/d_o$. Values taken from a table in [9] indicate that, in current heat exchanger design practice, this dimensionless clearance parameter lies between 0.00625 and 0.064. The variation of the depth of rolling is considered by varying the ratio l/h. The case where $l/h > 1.0$ cannot be treated by the present computer program.

5.2 Degree of Expansion. The resulting state of the residual stress depends on one additional parameter, which describes the degree of expansion of the tube. This parameter must be related to the maximum deformation induced in the tube-tubesheet assembly after expansion. The useful degree of expansion lies between two limits. At the lower limit, the gap between the tube and the hole is just closed. The upper limit is based on either the axial extrusion of the plastic tube material or excessive plastic deformation of the tubesheet.

The special-purpose computer program, KshelTZ, which was developed for this problem, calculates the two limits and displays their values on the screen. This gives the analyst the opportunity to select one or more intermediate values of the degree of expansion that lie between the lower and upper limits. After a level of the degree of expansion has been selected, KshelTZ then displays the predicted residual stresses and the changes in the geometry that would have been produced by

opment of the model, and they impose certain limitations on the validity of the model, if it is applied to a real expansion process. The lifting of any one of these assumptions would make the model more complicated. The authors believe that a model that makes these assumptions can still capture the gross features of the expansion process.

Regarding the first assumption, roller expansion is clearly not an axisymmetric process. Regarding the second assumption, the exact slope at the junction depends on local properties that are difficult to predict. The effects of roller and hydraulic expansion on this slope may be quite different. Regarding the third assumption, its effect is expected to be small because the portion of the expansion force represented by Q is only a small fraction of the total expansion force.

However, in both roller and hydraulic processes, the inaccuracies introduced by the three assumptions are expected to be in the proximity of the toe and to decay when going away from the toe. For this reason, the model is expected to be more reliable in the tail of the transition zone than in the toe. Moreover, if stress corrosion cracking is of concern, then any theoretical analysis in the toe may be inadequate for the rolling process, because the surface in the toe may have suffered mechanical damage by contact with the ends of the rollers. This damage may be sensitive to the shape of the ends, the number of rollers, the degree to which the joint has been rolled, and perhaps other parameters. The effect of this damage on crack initiation and growth is not easily predictable.

4 Mathematical Model

The analysis treats the movement and stress history of three separate parts: 1) tubesheet, 2) uniformly expanded zone of the tube, and 3) transition zone of the tube. The behavior of each part during the load-up and springback phases is considered using the appropriate nondimensional variables. Equilibrium and compatibility of the parts are enforced using the dimensional variables.

4.1 Analysis of Tubesheet. The tubesheet is treated as an elastic-plastic annular flat plate of inner radius a, outer radius b, and thickness h. It is subjected during loading to a radially outward load of N per unit circumference at the inner edge while it is free at the outer edge. It is assumed that only in-plane deformation occurs and that the stress in the axial direction is zero. At the state of maximum radial expansion the load N reaches the value $\hat{N}$ while the radial displacement at the edge of the hole is $\hat{u}$. An elastic-linearly hardening model with Young's modulus E', yield stress Y', and tangent modulus $E'_{\tan}$ is used. The behavior of the model of the tubesheet is presented in terms of the nondimensional variables a/b, $E'_{\tan}/E'$, $\hat{N}/Y'h$, and $E'\hat{u}/Y'a$. Thus, for given ratios a/b and $E'_{\tan}/E'$, curves of $\hat{N}/Y'h$ versus $E'\hat{u}/Y'$ are calculated by incremental elastic-plastic analysis. Points on these curves are stored in a data base so that curves for other values of a/b and $E'_{\tan}/E'$ may be obtained by interpolation from the data base. Having the load-displacement in nondimensional form, the dimensional relationship between $\hat{N}$ and $\hat{u}$ is obtained by multiplying the nondimensional variables by the appropriate size parameters for the tubesheet.

During removal of the expander, the tubesheet springs back, so that the material unloads elastically. Letting $\bar{N}$ be the change in radial load and $\bar{u}$ be the change in radial displacement at the hole during unloading, the relation between $\bar{u}$ and $\bar{N}$ is calculated from the familiar formula

$$\bar{u} = (\bar{N}a/E'h)[(b^2+a^2)/(b^2-a^2)+\nu'] \tag{1}$$

from elastic analysis of a thick-walled cylinder. The residual values are $\tilde{N}$ and $\tilde{u}$ given by

$$\tilde{N}=\hat{N}+\bar{N},\ \tilde{u}=\hat{u}+\bar{u} \tag{2}$$

4.2 Analysis of Uniformly Expanded Zone of Tube. Figure 4 depicts the loads acting on the expanded zone and the transition zone. Both the pressure p_i and the shear force Q are carried by the expander. The material constitutive relations are assumed to be elastic-linearly hardening in both zones.

If the loading for the expansion process is simulated by uniform pressure on the inner tube surface, the expanded zone of the tube behaves as a cylindrical tube under internal pressure while the gap between the tube and tubesheet is still open. After the gap is closed, a contact pressure develops between the tube and the tubesheet, so that the tube is then under internal pressure p_i and external pressure p_o. At this stage, the expanded zone is assumed to be fully plastic. The state of stress is then calculated using the equilibrium equation

$$d\sigma_r/dr = (\sigma_\theta - \sigma_r)/r \tag{3}$$

together with the von Mises yield condition

$$(\sigma_r^2 - \sigma_r\sigma_\theta + \sigma_\theta^2) = \sigma_{eq}^2 \tag{4}$$

The subsequent yield stress, σ_{eq}, which includes the effect of strain hardening is treated as constant through the tube thickness. A reasonable estimate of the equivalent yield stress σ_{eq} for the strain-hardened tube is obtained by using the plastic circumferential strain as the equivalent plastic strain. For a linearly hardening material, the equivalent stress can be approximated by

$$\sigma_{eq} = Y + E_{\tan}(\hat{w}/R - Y/E) \tag{5}$$

The solution to the differential Eq. (3) obtained by using the boundary conditions $\sigma_r = -p_i$ at $r=r_i$ and $\sigma_r = -p_o$ at $r=r_o$ then provides a relationship between p_i/σ_{eq} and p_o/σ_{eq} in terms of the radius ratio r_o/r_i.

If unloading behavior of the expanded zone is assumed elastic, then the change in displacement at the outer tube surface is given by the thick-walled cylinder formula

$$\bar{u} = 2\bar{p}_i r_o r_i^2/(r_o^2 - r_i^2)E - \bar{p}_o r_o[(r_o^2+r_i^2)/(r_o^2-r_i^2) - \nu]E \tag{6}$$

Since yielding may occur in the expanded zone upon unloading, it is necessary to check the residual stresses to be sure that they lie within the strain-hardened yield surface. If it is determined that yielding occurs, then (6) is replaced by the condition that the residual stress state lies on the yield surface.

4.3 Analysis of Transition Zone. The mathematical model for a cylindrical shell of elastic-plastic material is used. Boundary conditions model the applied edge displacements at the attachment to the expanded zone and the stiffness of an attached semi-infinite elastic cylindrical shell at the other end. Its edge is subjected to an outward displacement while the expansion loading is applied, and a springback displacement when it is removed. It is also assumed that the expander and tubesheet provide sufficient constraint that the displaced edge undergoes zero rotation, and that the process causes no buildup of axial force in the shell. The loads on the transition zone consist of the edge shearing force Q and the edge bending moment M shown in Fig. 4(*b*). During the outward expansion phase, the material behavior is taken to be elastic-linearly hardening with Young's modulus E, yield stress Y, and tangent modulus $E_{\tan}$. Elastic unloading is assumed during springback.

The nondimensional variables used in the analysis are the displacement Ew/YR, the stress σ_x/Y and σ_θ/Y, the distance along the tube $x/\sqrt{(Rt)}$, the edge radial shear $Q\sqrt{(Rt)}/Yt$, and the bending moment M/Yt^2. The KshelPL computer program, which performs incremental elastic-plastic analysis of thin shells of revolution under axisymmetric loading [7], has been used to calculate the relationship between the nondimensional shear force and the nondimensional edge displacement at a few levels of $E_{\tan}/E$. The results of the calculations have been tabulated and stored in a data base for later use. Linear interpolation is used to obtain the curves for inter-

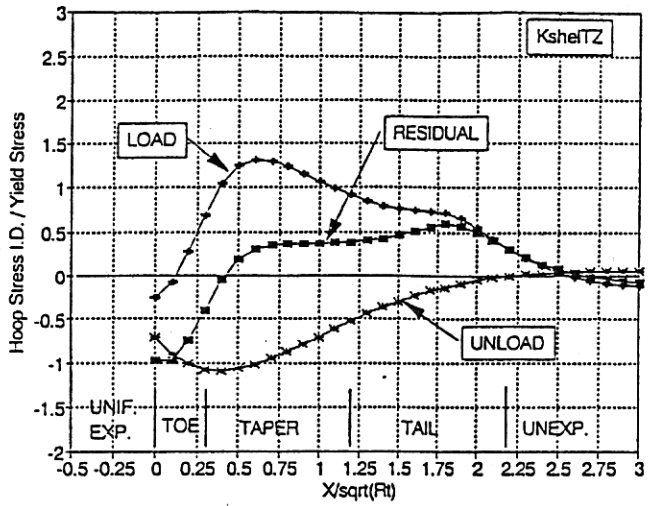

Fig. 7 Distributions of hoop stresses on inside diameter for reference

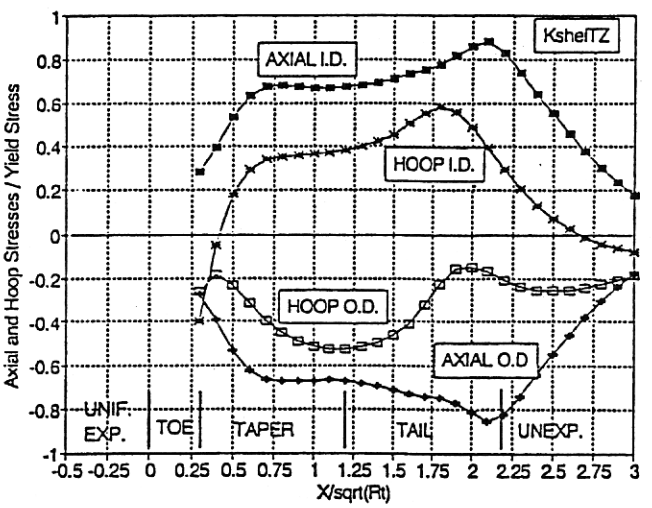

Fig. 8 Distributions of residual stresses on inside and outside diameters for reference case

8.2 Hoop Stress. The corresponding hoop stresses on the inside diameter are shown in Fig. 7. Because of the large axial stress in the toe during load-up, the hoop stresses are depressed by the yield condition to a negative value, as shown by the curve LOAD. If the axial stresses at the junction are judged unreliable, then the sharp decrease in hoop stress in the toe may also be unreliable. It may be noted that in the taper zone the maximum hoop stress upon load-up is at about the same level as the maximum axial stress in the tail, but in the taper the unload stress is more severe, so that the residual hoop stresses remain below the residual axial stresses.

8.3 Effect of Residual Stresses on Stress Corrosion. Figure 8 shows the residual axial and hoop stresses on the inside diameter that are predicted for the reference case at the apparent wall reduction of 5 percent. It is seen that the tensile residual axial stresses exceed the hoop stresses. Even with a more accurate consideration of the severe bending at the junction the uniformly expanded zone and the toe, it is not likely that the hoop stresses will be higher than the axial stresses. While this result is also shown for calculated stresses in Fig. 4 of [5], and for measured stresses in Fig. 6 of [6], it may be contested by other investigators.

When applied to a real expansion process, this result suggests that, all other things being equal, circumferential stress corrosion cracks should predominate on the inside diameter of the tube. However, reports from other investigations, such as [5], show axial stress corrosion cracks in the toe that turn into circumferential cracks in the tail. It may be difficult to reconcile the presence of axial cracks on the basis of results of the model that is presented in this paper, because this model takes into account only residual stresses that are left in the tube by the expansion process, while other parameters, including residual stresses from other sources, may be at work when the cracks are produced.

Table 1 Maximum axial residual stress on inside diameter

Parameter	Low	Ref.	High	Result
t/d_o	0.0333	0.0667	0.133	Fig. 9
b/a	1.6	2.0	3.0	Fig. 10
Y'/Y	0.8	1.0	1.25	Fig. 11
$2c/d_o$	0.0063	0.02	0.064	See text
$h/2a$	0.5	1.0	2.0	No change
E_{tan}/E		0.01	0.02	No change
E'_{tan}/E'		0.01	0.02	No change

Owing to the result that the axial residual stresses are greater than the hoop stresses, the following parameter study will be restricted to axial residual stresses on the inside diameter.

9 Parameter Study for Axial Stresses

This section presents results obtained by varying selected tube and tubesheet parameters, one at a time. Attention is focused on how the maximum residual axial stress on the inside diameter varies with the apparent wall reduction. In each case, the parameters of the reference case are used, with the varying parameter being assigned values above and below that of the reference case. The results of the parametric study are shown in Table 1.

Regarding Table 1, "no change" means that, between the low and high values considered, there was hardly any change in the maximum residual stress values for the range of apparent wall reduction between 2 and 8 percent.

The effect of the initial clearance between the tube and the tubesheet requires a special discussion. The effect was studied for the range between $2c/d_o = 0.00625$ and 0.064, which was consistent with the clearances specified in the TEMA standards [9]. These values include classes "C," "R," and "B" of TEMA heat exchangers. For the closest fit ($2c/d_o = 0.00625$), the residual axial stress at the inside diameter was about $0.77Y$ to $0.81Y$. For the loosest fit ($2c/d_o = 0.064$), the calculations indicated an axial residual stress of $1.30Y$. The reason why clearance has a large effect on the residual stresses is that, during the load-up, the material strain-hardens as the gap is closed. The larger the gap, the more strain hardening. Thus, for larger gaps, the material unloads from higher stress values. Since the unloading is elastic, the residual stress magnitude could be as high as $1.30Y$. The calculations for the loosest fit led to plastic strains in the tube lying outside the data base of KshelTZ. Moreover, the use of a linear hardening law in this case may not be justified. For these reasons, the graphs are not shown.

10 Discussion

In all of the cases studied, the maximum axial stress at the inside diameter in the transition zone lies in the range of 77 to 95 percent of the tube yield stress. This range is achieved independently of the geometric and material specifications of the joint. Even when the apparent wall reduction is well beyond the 5 percent optimum value recommended in [12], the residual stresses lie within this range.

Why does the residual stress always lie in this range for so many of the cases, and where in the transition zone does the maximum of this stress occur? The location of this maximum is near the end of the penetration of the plastic zone into the

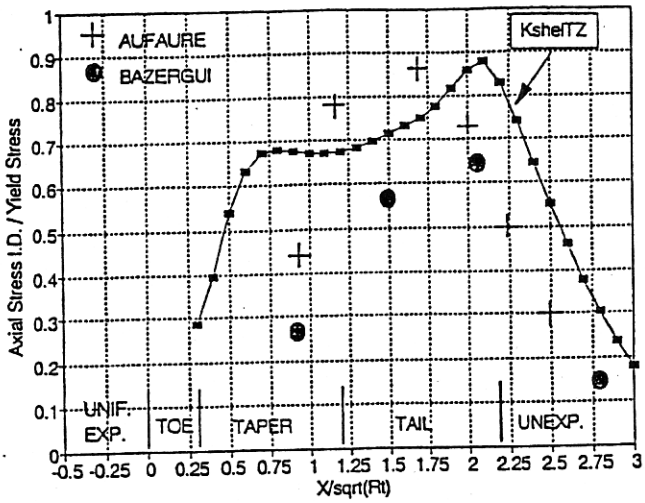

Fig. 5 Distribution of residual axial stress in transition zone

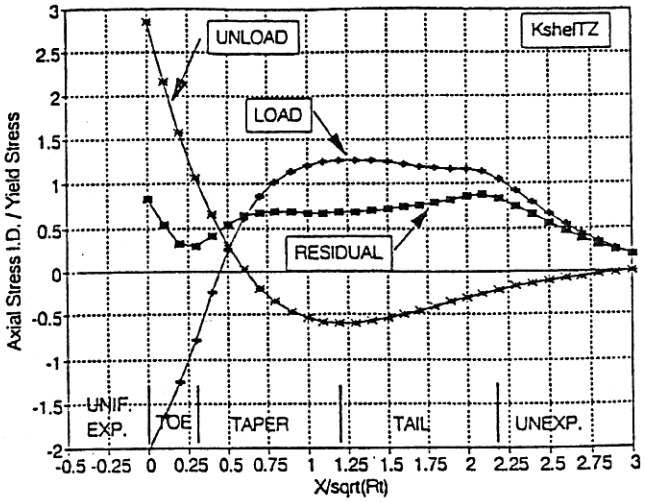

Fig. 6 Distributions of axial stresses on inside diameter for reference case

the expansion process. By changing the level of the degree of expansion, the analyst can relate the optimum residual stresses with the final geometry of the tube-tubesheet assembly.

The measure that can be used to represent the degree of expansion has been much debated in the literature. Fisher and Cope [10] discuss three methods and propose a fourth one, which they call the elongation method. As the tube material is squeezed between the expanding tool and the hole, it moves axially (elongates the tube). The degree of expansion is assessed by the magnitude of the elongation. Grimison and Lee [11] report experimental results in their Figs. 4 and 5 that are plotted against both "the percent total extrusion," which is the elongation method, and the "percent increase in tube inside diameter over that at contact at seat," which is what is called by Yokell (see [2, p. 83]) the "apparent wall reduction." This is also the measure that is used by a major manufacturer of heat exchanger and condenser tube expanders [12]. (In order to achieve an "optimum" joint, it is recommended in [12] that the apparent wall reduction be held between 4 and 5 percent.) The apparent wall reduction is adopted here as the measure of the degree of expansion of the tube.

Grimison and Lee [11] define the apparent wall reduction as ". . . the percentage increase in the inside diameter of the tube over that calculated at first uniform contact of tube and seat . . .". Denoting the apparent wall reduction by m, then

$$m = [d_i' - (d_i + 2c)]/2t \tag{20}$$

where d_i' is the measured, final inside diameter of the tube, d_i is the inside diameter of the unrolled tube, and $2c$ is the diametral gap between the tube and the hole. If expressed as a percentage, m is multiplied by 100.

6 Reference Case

The dimensionless parameters used for this case are

$$t/d_o = 0.0667, \quad E/Y = 1000, \quad E_{\tan}/E = 0.01$$
$$b/a = 2.0, \quad h/2a = 1.0$$
$$Y'/Y = 1.0, \quad E'/E = 1.0, \quad E_{\tan}'/E' = 0.01$$
$$2c/d_o = 0.02, \quad l/h = 1.0$$

This case is representative of many tube-tubesheet joints encountered in engineering practice. Both the tube and the tubesheet are assumed to have the same stress-strain curve. The E/Y ratio is representative of low strength and stainless steels.

7 Comparison With Experimental Data

For comparison with reported experiments, the residual stresses on the inside diameter of the reference case are plotted in Fig. 5. The curve shows the distribution of the stress in the taper of the transition zone of the tube. The experimental results that report axial stresses are taken from [5 and 6]. The agreement appears to validate the mathematical model developed in this paper.

Regarding the experimental data, it was difficult to establish the exact location of the junction between the uniformity expanded zone and the toe. For this reason, the experimental points could be moved to the right or left. Furthermore, the geometric and material data in the experiments did not match those of the reference case. The data were transferred to Fig. 5 in terms of the same nondimensional variables as those of the reference case.

8 Residual Stress Magnitudes on Inside Diameter

The mathematical model described in the foregoing has been incorporated in an interactive computer program, called KshelTZ. This program was used to run many cases. As an example of the results given by KshelTZ, the stress distributions were obtained for the reference case at the apparent degree of expansion of about 5 percent. Qualitatively similar results were obtained for other cases. We shall discuss some of these results.

8.1 Axial Stress. The load, unload, and residual axial stresses are shown in Fig. 6. The LOAD curve in Fig. 6 is shown to go to $-2.0Y$ at the junction between the uniformly expanded zone and the toe. The high stress comes from large axial bending strains and severe strain-hardening at the junction. The large strains come from the severe bending that is enforced at the junction by the assumed zero slope. The strains at the junction may not be accurate, which renders the LOAD stresses at the junction also inaccurate. For this reason, the residual stresses in the toe should not be regarded as reliable.

Referring again to Fig. 6, it is seen that in the tail of the transition zone, from $x/\sqrt{(Rt)} = 1.2$ to 2.0, the LOAD stresses are limited by the strain-hardened yield condition to about $1.2Y$. It is also seen that elastic UNLOAD stress diminish rapidly from $x = 0$, so that at $x/\sqrt{(Rt)} = 2.0$ the unloading stress magnitude is only $0.3Y$. This explains why the residual axial stresses are about $0.9Y$. If the tube is expanded more than the apparent wall reduction of 5 percent, the tail is pushed further out, beyond $x/\sqrt{(Rt)} = 2.0$, while the stress level remains about the same, at $1.2Y$. Then unloading makes even a smaller contribution, and the residual stress is higher than $0.9Y$. This explains why the maximum axial residual stress should rise slightly with the apparent wall reduction.

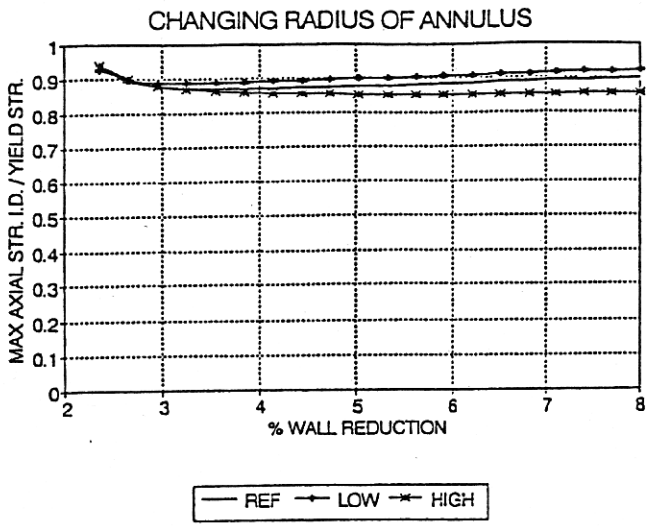

Fig. 9 Variation of maximum axial residual stresses versus apparent wall reduction for different annulus radii

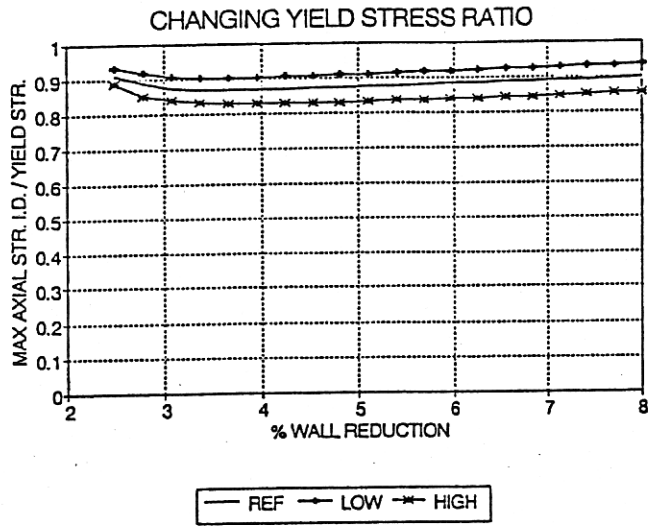

Fig. 10 Variation of maximum axial residual stresses versus apparent wall reduction for different tube thicknesses

transition zone during the expansion. For a perfectly plastic, semi-infinite cylindrical shell, loaded to the limit state by edge loads, the plastic zone ends at the state of stress corresponding to a hinge circle. For a material that satisfies the Tresca yield condition, the location of the hinge circle can be calculated using the equations derived in [13]. For edge loading similar to that produced by the expander, the distance from the edge of the roller to the hinge circle is calculated to be about $1.2\sqrt{(Rt)}$. The bending stress at the hinge circle is equal to Y for the Tresca yield condition and $1.155Y$ for the von Mises yield condition. A stress field that extends into the rigid region, beyond the hinge circle, may consist of a finite length of shell over which the same stress state occurs. In the present elastic-plastic expansion analyses for a material with a very small amount of strain hardening, the calculated stresses approximate this condition. With increasing expansion, this finite zone of material with high bending stress spreads beyond the $1.2\sqrt{(Rt)}$ circle, in some cases going beyond a distance of $2.0\sqrt{(Rt)}$.

When the loading is released, the tubesheet provides a springback force. This springback action causes only elastic changes in the transition zone. It is well known that elastic shell solutions for cylindrical shells decay rapidly with the distance

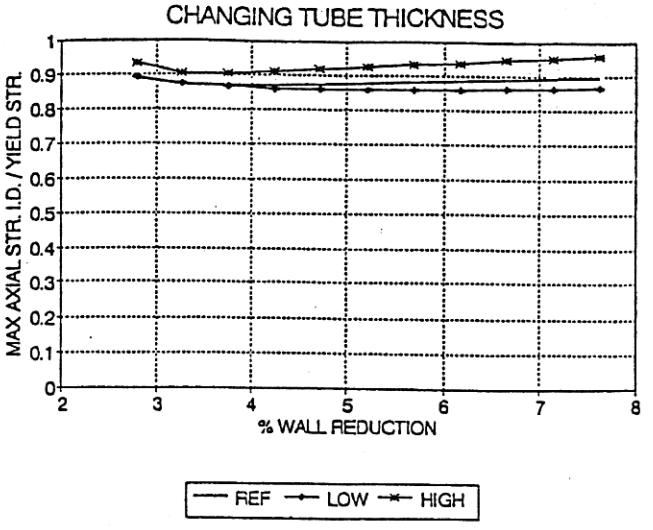

Fig. 11 Variation of maximum axial residual stresses versus apparent wall reduction for different yield stresses

from the edge loading; therefore, the stress release at a distance of 2.0 time $\sqrt{(Rt)}$ from the edge is small.

In summary, the explanation for the consistent value of residual stress at the inside diameter is simply this. During expansion, the tube bending stress must reach about $1.1Y$ in order to expand the tube into the tubesheet. During springback, only about $0.25Y$ is released leaving a residual stress of about $0.85Y$. The foregoing discussion also shows that the maximum tensile axial residual stress occurs at a distance of about 1.2 to 2.0 times $\sqrt{(Rt)}$. With this explanation, it is now apparent why the clearance alone had a significant effect on the axial stress. For the very loose fit, the tube strain-hardens as it is expanded to close the gap. Then, upon unloading, the stress is released from a much higher value, which results in a higher residual stress. This means that it is possible to account for the clearance by considering the strain-hardening that takes place as the tube is expanded to close the gap. Of course, any limits on material ductility must also be taken into account in the case of a very loose fit.

11 Conclusions

The mathematical model developed in this paper provides estimates of residual stresses that are left in an expanded tube by the expansion process. The residual stresses agree qualitatively with experimental values reported in [5 and 6]. Using the calculation procedure, the tubes stresses can be compared with the threshold values of the stresses for stress corrosion cracking in a proposed tube-to-tubesheet joint.

Expansion of tubes to provide tube-to-tubesheet contact pressure can lead to tensile residual stresses in the transition zone of the tube. A tensile stress of 90 percent of yield stress or higher may occur. Under some environments, these residual stresses, when added to other stresses that are present, may produce resultant stresses above the threshold value for stress corrosion cracking in the tube.

For the geometric and material parameters that were investigated, the model predicted the maximum tensile stresses to be axial and located on the inside diameter of the tube.

References

1 Goodier, J. N., and Schoessow, G. G., "The Holding Power and Hydraulic Tightness of Expanded Tube Joints: Analysis of the Stress and Deformation," TRANS. ASME, 1943, pp. 489–496.

2 Yokell, S., "Heat-Exchanger Tube-to-Tubesheet Connections," *Chemical Engineering*, February 8, 1982, pp. 78–94.

3 Soler, A. I., and Hong, Xu., "Analysis of Tube-Tubesheet Joint Loading

Including Thermal Loading," ASME *Journal of Applied Mechanics*, Paper No. 84-APM-15, 1984.

4 Jawad, M. H., Clarkin, E. J., and Schuessler, R. E., "Evaluation of Tube-to-Tubesheet Junctions," ASME JOURNAL OF PRESSURE VESSEL TECHNOLOGY, Vol. 109, Feb. 1987, pp. 19–26.

5 Druez, J., Bazergui, A., and Pettigrew, M. J., "Residual Stresses in Roller-Expanded Thin Tubes," *Experimental Mechanics*, Vol. 24, 1984, pp. 316–324.

6 Aufaure, M., Boudot, R., Zacharie, G., and Proix, J. M., "Analysis of Residual Stresses due to Roll-Expansion Process: Finite Element Computation and Validation by Experimental Tests," *Trans. of the 9th International Conference of SMiRT*, Vol. B, Aug. 1987, pp. 499–503.

7 Updike, D. P., and Kalnins, A., "Elastic-Plastic Analysis of Shells of Revolution Under Axisymmetric Loading," *WRC Bulletin 364*, June 1991.

8 Wang, Y., and Soler, A. I., "Effect of Boundary Conditions on the Tube-Tubesheet Joint Annulus Model—Finite Element Analysis," *Design and Analysis of Piping, Pressure Vessels, and Components*, ASME PVP-Vol. 139, eds., Q. N. Truong, G. N. Brooks, A. A. Dermenjian, and W. E. Short II, 1988, pp. 107–112.

9 Tubular Exchanger Manufacturers Association, Inc., *Standards of Tubular Exchanger Manufacturers Association*, Sixth Edition, 1988.

10 Fisher, F. F., and Cope, E. T., "Rolling-in of Boiler Tubes," TRANS. ASME, Vol. 57, 1935, pp. 145–152.

11 Grimison, E. D., and Lee, G. H., "Experimental Investigation of Tube Expanding," TRANS. ASME, Vol. 65, 1943, pp. 497–505.

12 Airetool Cleaners and Expanders Catalog, Industrial Tool Division, Dresser Industries, Inc. Union, N.J.

13 Ho, H. S., and Updike, D. P., "Limit Analysis for Combined Edge and Pressure Loading on a Cylindrical Shell," ASME *Journal of Engineering for Industry*, Vol. 93, 1979, pp. 998–1006.